Author Material: Text

Materials and Methods

Group matching algorithm

The TD cohort was selected by a customized matching algorithm from a larger sample of TD children who were part of an ongoing study at Stanford University. One of the co-authors (K.S.) developed an optimization method that uses the general properties of the experimental group in order to select a well-matched sample of TD individuals through the principles of genetic algorithms. For this study, the TD cohort was selected to be matched to the ASD group on age, full scale IQ and gender ratio as follows. Given the relevant criteria of the experimental group (in our case, gender ratio, age, and full-scale IQ mean and standard deviation of the ASD group), the algorithm randomly creates 10,000 combinations of 20 individuals each (i.e. the size of the experimental group) and computes a fitness score (as intended by genetic algorithms and thereby in biological terms) for each of the created combinations. The fitness score is then entered into a ruler probability distribution to find, using crossing-over on the pairs that best matched a subset of participants (i.e. how well the fitness score of each of the created combinations matches the original criteria), the optimal TD group. This algorithm is designed to be less biased than most common matching criteria (i.e. one to one matching) which make the assumption that each individual in the experimental population is identical to their control subject with the only exception that the latter does not present a clinical characteristic (e.g. ASD).

fMRI data preprocessing

A linear shim correction was applied separately for each slice during reconstruction using a magnetic field map acquired automatically by the pulse sequence at the beginning of the scan [1]. Functional MRI data were then analyzed using SPM8 analysis software (http://www.fil.ion.ucl.ac.uk/spm). Images were realigned to correct for motion, corrected for errors in slice-timing, spatially transformed to standard stereotaxic space (based on the Montreal Neurologic Institute (MNI) coordinate system), resampled every 2 mm using sinc interpolation and smoothed with a 6mm full-width half-maximum Gaussian kernel to decrease spatial noise prior to statistical analysis. Translational movement in millimeters (x, y, z) and rotational motion in degrees (pitch, roll, yaw) was calculated based on the SPM8 parameters for motion correction of the functional images in each subject. In both groups, average movement was less than 0.5 mm root mean square (RMS), and RMS values did not differ between children with ASD and TD children (ASD: 0.3 ± 0.2; TD: 0.4 ± 0.3, $p > 0.5$). No subject displayed greater than 5mm translational motion or greater than 5 degrees rotational motion (ASD: range x = 0.58 ± 0.64, range y = 0.80 ± 0.55, range z = 1.75 ± 1.21, range pitch =1.74 ± 0.94, range roll = 0.84 ± 0.57, range yaw = 0.63 ± 0.52; TD range x = 0.53 ± 0.33, range y = 0.89 ± 0.93, range z = 1.58 ± 1.35, range pitch = 1.72 ± 1.26, range roll = 0.86 ± 0.81, range yaw = 0.75 ± 0.68, all $p > 0.5$).

Dual regression ICA

Independent component analysis (ICA) is a model-free, data-driven approach whereby four-dimensional fMRI data is decomposed into a set of independent one-dimensional timeseries and associated three-dimensional spatial maps, which describe the

temporal and spatial characteristics of the underlying signals or components [2]. In the dual regression approach (http://www.fmrib.ox.ac.uk/analysis/dualreg/), preprocessed data from all participants are first entered into a group ICA to identify large-scale patterns of functional connectivity in the population. In the current study, we decomposed the data into 25 independent components and selected ten components corresponding to previously described functional networks, as described.

Next, the dual-regression algorithm was applied to identify subject-specific timecourses and spatial maps. This procedure employs a set of ICA spatial maps derived from the initial group ICA in a linear model fit against each individual fMRI dataset, resulting in matrices describing the temporal dynamics of the corresponding networks for each subject. The timecourse matrices are normalized by their variance and used in a linear model fit against each individual fMRI dataset. This temporal regression results in subject-specific spatial maps that reflect degree of synchronization (both amplitude and coherence across space [3, 4]). The different synchronization maps were then collected across subjects into 4D files (one per original ICA map), and submitted to voxel-based statistical testing using nonparametric permutation testing [5]. Group difference maps from this statistical testing were thresholded at the $p < 0.05$ level, as described in the text.

Background: Sparse linear classification and regression

In this study we used sparse logistic regression for classification and sparse linear regression for exploring relationships between brain networks and ASD symptom severity. We used the Matlab package GLMnet (http://www-stat.stanford.edu/~tibs/glmnet-matlab) to implement these two methods. First, we used a

sparse logistic regression classifier to classify children with ASD and TD children using network measures derived from dual regression. Next, we applied sparse linear regression to investigate whether measures of network connectivity predict symptom severity in ASD. In this study, conventional methods for classification and regression would have resulted in over-fitting because the predictors (number of voxels within each network) outnumber the available observations (number of subjects). The sparse methods that we used in this study overcome this problem by using regularization. Using GLMnet one can apply either lasso (or L1-norm) or elastic net (a combination of L1 and L2-norm) regularization [6]. This regularization not only overcomes the problem of over-fitting but also provides sparse solutions, which will be useful in finding brain regions that discriminate between ASD and TD children in the case of classification and the brain regions that predict symptom severity in ASD. In the current study, we applied sparse methods with lasso regularization to avoid over-fitting and were not intending to identify specific brain regions within networks. The lasso penalty (L1-norm), which we used here is not suitable for identifying specific voxels in the brain in cases like ours, wherein the predictors outnumber the observations. In such situations, this approach has the following limitations [7]:

(a) When the number of predictors (p) is larger than the number of observations (N), lasso can at most discover N predictors.

(b) If the pairwise correlations between the predictors are high (which is generally true in neuroimaging data because of high spatial correlations) lasso tends to select only one predictor among the relevant predictors. Lasso regularization does

not care which one is selected, and also the selected predictor can vary if the algorithm is run multiple times.

Therefore, discovering specific brain regions within networks in these two analyses is not reliable using lasso regularization. However, these two limitations can be overcome by using elastic net regularization. Elastic net regularization is more suitable in cases where identifying specific brain regions is the main focus of the study. Future work will explore such regularization approaches.

Network-based classification: Logistic regression with lasso regularization

The ten components identified from each individual subject by the dual regression analysis served as features to be input into classification analyses. For these analyses, individual subject maps for each network were masked with the corresponding network originally derived from the group ICA (thresholded at $z > 4.3$, $p < 0.0001$). For classification, we used a logistic regression classifier with lasso regularization. We used the Matlab package GLMnet (http://www-stat.stanford.edu/~tibs/glmnet-matlab) to fit the classifier. We estimated the classification accuracy using a Leave-One-Out Cross Validation (LOOCV) procedure. In LOOCV, data are divided into N folds (here, N = 40). A classifier is built using N-1 folds, leaving out one sample. The left out sample is then classified using this classifier, and the classification accuracy is noted. The above procedure is repeated N times by leaving out one sample each time, and finally an average classification accuracy is computed on left out folds. This value is termed cross validation accuracy, which we report alongside sensitivity, specificity, PPV and NPV for each of the ten networks. Permutation tests (10,000 permutations of class labels for each

network) were conducted to arrive at *p*-values associated with classification accuracies for each network.

To test whether the classifier developed based on the current dataset could generalize to a novel dataset, we conducted a dual regression analysis on an independent dataset (ASD n = 15, TD n = 15) obtained from publicly available databases (described below). Using the salience network template from the original dataset, dual regression was performed on the independent dataset to derive features for classification analyses.

Results

Comparable large-scale brain networks in children with ASD and TD children examined separately

In order to compare brain networks between two groups, it is necessary that the networks of interest should be present in both groups separately for meaningful comparisons to be carried out. To confirm that the ASD and TD groups each separately contained the networks present in the group ICA merging all datasets together (ASD + TD, **Fig. 1**), we conducted separate ICA analyses of the ASD and TD groups. These analyses suggest that the networks are indeed comparable in ASD and TD. With the exception of the visual association network, which was absent in the TD group, all other networks of interest were observed in the ASD and TD groups separately. It is also worth noting that the dorsal attention network appeared slightly different in terms of spatial extent in the ASD and TD groups analyzed separately (**eFig. 1, eFig. 2**).

Robustness of findings to motion artifacts

It has recently been demonstrated that subject motion can induce spurious correlation structures in resting state fMRI[8]. We applied the "data scrubbing" method

proposed by Power and colleagues to ensure that motion artifacts were not contributing to the group differences we observed. Prior to the dual regression step, for each participant, volumes with framewise displacement greater than 0.5 mm and derivative variance greater than 0.5% of BOLD signal were identified and excluded, using the parameters proposed in [8]. As can be seen in **eFig. 3**, the group difference results are not changed by the scrubbing procedure. Of note, in addition to the ASD > TD findings we originally report, the scrubbing analysis uncovers an additional ASD > TD finding in the dorsal attention network (albeit a very small cluster, not shown). This analysis confirms the robustness of our initial findings.

Replication Analyses

Fifteen children with ASD and 15 age-, gender-, and IQ-matched TD children were identified from public domain research data repositories. Specifically, children with ASD were identified by querying the National Database for Autism Research repository (NDAR; http://ndar.nih.gov) using the following query parameters: age 7-13; phenotype ASD; resting state fMRI data present. This query yielded 15 children with ASD (11 male, 4 female) ranging in age from 8 to 13 years (10.38 ± 1.34) with a full-scale IQ range of 73 to 132 (98.6 ± 18.8). Notably, all of the subjects identified belong to one collection submitted by F. Xavier Castellanos at New York University. This collection did not include data from TD children. To address this issue, we queried the ADHD200 dataset (http://fcon_1000.projects.nitrc.org/indi/adhd200/) which contains resting state fMRI data from TD children and children with attention-deficit/hyperactivity disorder (ADHD) across 8 different sites including Dr. Castellanos' lab at NYU. The query parameters were: site NYU, age 7-13, phenotype TD, resting state fMRI data present. The query

yielded 60 TD children. We used an in-house matching algorithm (described above, *Group matching algorithm*) to select a subset of 15 TD children such that the mean age, mean full-scale IQ, and gender distribution were matched to the ASD group. The algorithm identified a well-matched subset of 15 TD children (11 males, 4 females) ranging in age from 7 to 13 years (10.23 ± 1.65) with an IQ range of 80 to 142 (107 ± 18.2). Note that IQ data were available for 12 out of 15 children with ASD in this cohort, and ADOS and ADI data were available for 10 out of 15 (ADOS Social: 6.8 ± 1.3; ADOS Comm: 3.3 ± 1.5; ADI-A: 17.3 ± 5.1; ADI-B: 14 ± 2.8; ADI-C: 3.2 ± 1.3).

Data analysis was conducted in an identical manner to that described in the main manuscript in terms of preprocessing and dual regression ICA. We observed 13 components of interest in the combined group ICA of this independent dataset (**eFig. 4**). Some of the components initially observed in the original dataset were shown to split in the replication dataset. Specifically, the salience network appeared to split into separate anterior cingulate and anterior insular components, while the central executive network could be see as separate right and left components. In all of these components, ASD > TD connectivity was observed (**eFig. 5**). A few extra-network voxels were observed in two networks for the TD > ASD contrast.

Using the classifier built from the original data, we next tested whether ASD and TD could be discriminated in the independent dataset. For the salience network, 83% accuracy with 67% sensitivity and 100% specificity (PPV 100%, NPV 75%) was observed.

References

1. Glover GH, Law CS. Spiral-in/out BOLD fMRI for increased SNR and reduced susceptibility artifacts. *Magn Reson Med.* Sep 2001;46(3):515-522.

2. Beckmann CF, DeLuca M, Devlin JT, Smith SM. Investigations into resting-state connectivity using independent component analysis. *Philos Trans R Soc Lond B Biol Sci.* May 29 2005;360(1457):1001-1013.

3. Roosendaal SD, Schoonheim MM, Hulst HE, et al. Resting state networks change in clinically isolated syndrome. *Brain.* Jun 2010;133(Pt 6):1612-1621.

4. Westlye ET, Lundervold A, Rootwelt H, Lundervold AJ, Westlye LT. Increased hippocampal default mode synchronization during rest in middle-aged and elderly APOE epsilon4 carriers: relationships with memory performance. *J Neurosci.* May 25 2011;31(21):7775-7783.

5. Nichols TE, Holmes AP. Nonparametric permutation tests for functional neuroimaging: a primer with examples. *Hum Brain Mapp.* Jan 2002;15(1):1-25.

6. Hastie T, Tibshirani R, Friedman J. *The Elements of Statistical Learning: Data Mining, Inference, and Prediction.* Vol Second Edition. New York, NY: Springer; 2009.

7. Zou H, Hastie T. Regularization and variable selection via the elastic net. *Journal of Royal Statistical Society: Series B Stat. Methedology.* 2005;67(2):301 - 320.

8. Power JD, Barnes KA, Snyder AZ, Schlaggar BL, Petersen SE. Spurious but systematic correlations in functional connectivity MRI networks arise from subject motion. *Neuroimage.* Feb 1 2012;59(3):2142-2154.

eTable 1: Additional Participant Demographics

	ADOS-S	ADOS-C	ADI-A	ADI-B	ADI-C	Full-scale IQ	Current Medication Status	DSM-IV ADHD Problems	DSM-IV Anxiety Problems
ASD 1	5	2	26	20	6	98		Clinical Range	Borderline Clinical Range
ASD 2	11	7	24	14	8	94	Claritin, Benadryl for allergies	Normal Range	Normal Range
ASD 3	7	2	10	6	2	111		Normal Range	Normal Range
ASD 4	9	4	19	16	2	137	Sertraline, Risperidone	Clinical Range	Clinical Range
ASD 5	7	2	24	21	6	105	Zyrtec, Claratin for allergies	Normal Range	Borderline Clinical Range
ASD 6	7	6	21	22	11	78		Clinical Range	Borderline Clinical Range
ASD 7			27	20		100		Normal Range	Clinical Range
ASD 8	5	3	29	23	7	98		Normal Range	Normal Range
ASD 9	11	5	18	16	9	112	Zithromax 10 mg/ Lexapro 5 mg	Normal Range	Clinical Range
ASD 10	8	2	23	18	3	127		Normal Range	Borderline Clinical Range
ASD 11	11	5	16	10	6	97	Citalopram for social anxiety/ shyness	Normal Range	Clinical Range
ASD 12	10	5	26	22	6	141		Normal Range	Clinical Range

ASD 13	8	3	25	20	7	127		Normal Range	Borderline Clinical Range
ASD 14	8	2	13	11	3	124		Normal Range	Borderline Clinical Range
ASD 15	4	3	17	8	6	114	Adderall, Celexa, Risperidone, Invega	Borderline Clinical Range	Normal Range
ASD 16	9	5	21	11	6	107		Normal Range	Clinical Range
ASD 17	10	2	19	16	10	148	Concerta and Methylin	Clinical Range	Borderline Clinical Range
ASD 18	10	4	22	19	4	113	Zyrtec	Normal Range	Borderline Clinical Range
ASD 19	6	3	18	15	4	123	Singulair, zyrtec	Normal Range	Borderline Clinical Range
ASD 20	9	3	10	10	5	97	Tenex for tics (Tourette's)	Normal Range	Clinical Range

eFigure Captions

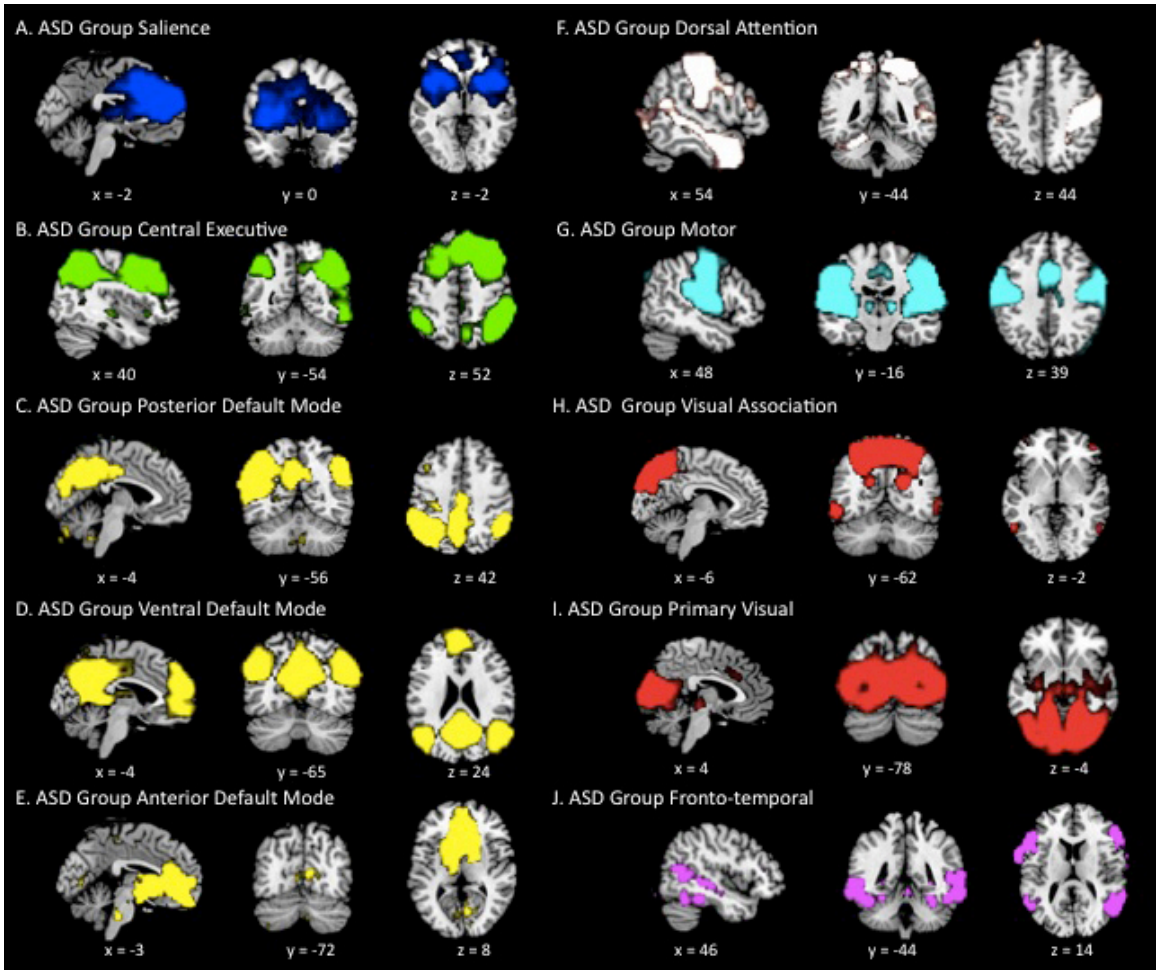

eFigure 1. Large-scale brain networks identified using ICA: ASD Group. Data from twenty children with ASD were combined in a group ICA to identify 25 independent components (networks) across all participants in a data-driven manner. Ten of these components correspond to previously identified functional networks: (a) salience; (b) central executive; (c) posterior default mode; (d) ventral default mode; (e) anterior default mode; (f) dorsal attention; (g) motor, (h) visual association, (i) primary visual, and (j) fronto-temporal. Maps are displayed at $z > 2.3$, $p < 0.01$.

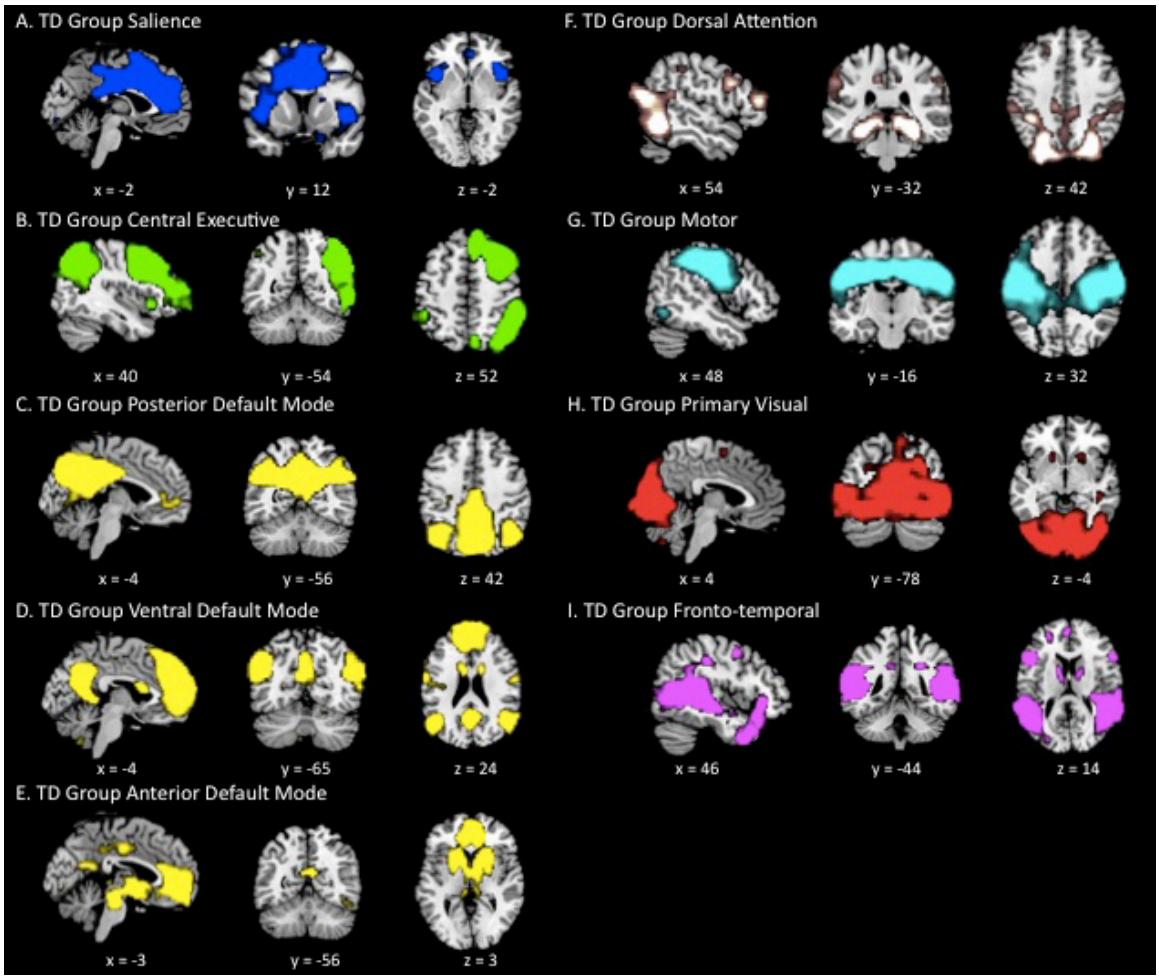

eFigure 2. Large-scale brain networks identified using ICA: TD Group. Data from twenty TD children were combined in a group ICA to identify 25 independent components (networks) across all participants in a data-driven manner. Nine of these components correspond to previously identified functional networks: (a) salience; (b) central executive; (c) posterior default mode; (d) ventral default mode; (e) anterior default mode; (f) dorsal attention; (g) motor, (h) primary visual, and (i) fronto-temporal. Maps are displayed at $z > 2.3$, $p < 0.01$.

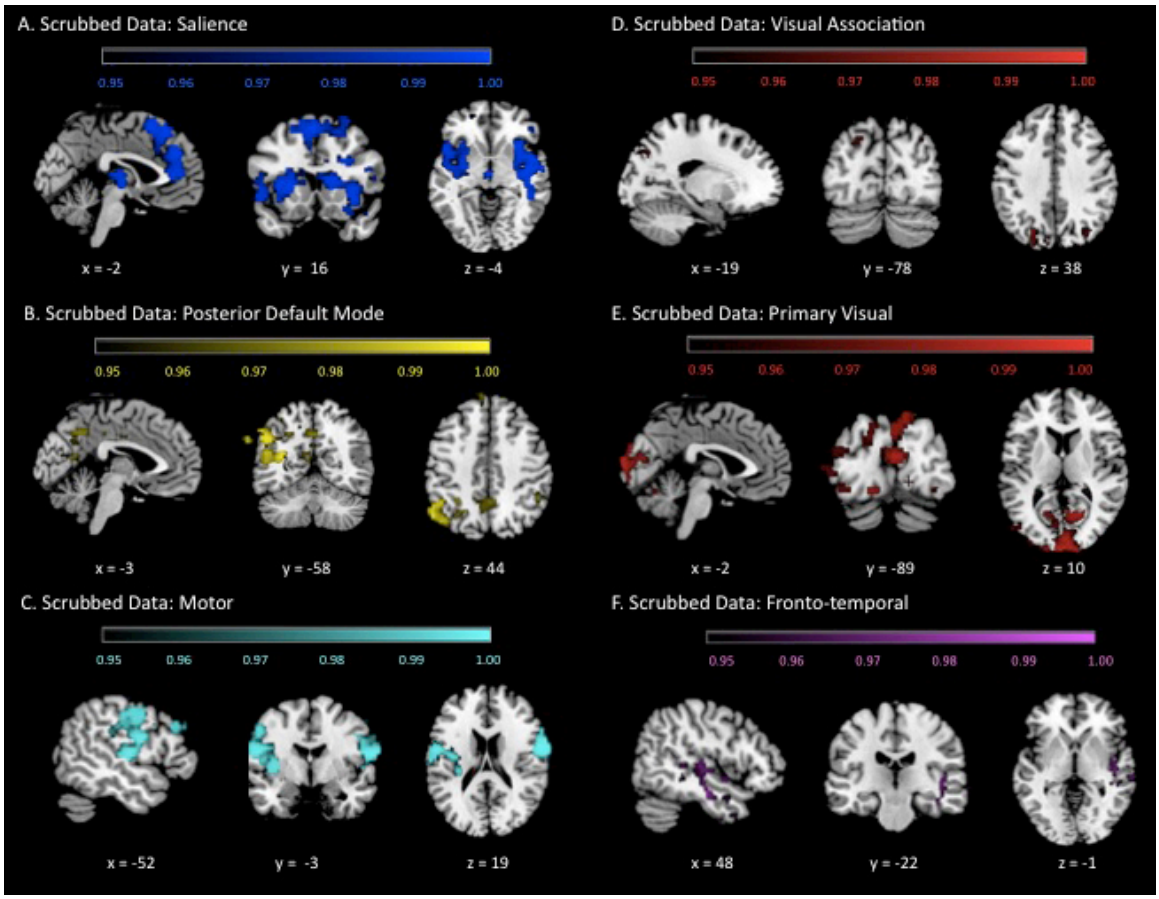

eFigure 3. Brain network hyper-connectivity in children with ASD: Scrubbed Data.

ASD > TD functional connectivity was observed in six of the ten networks examined: (a) salience; (b) posterior default mode; (c) fronto-temporal; (d) motor; (e) visual association; and (f) primary visual, even after removing individual frames with high motion. Group difference maps were thresholded using threshold-free cluster enhancement (TFCE) and $p < 0.05$.

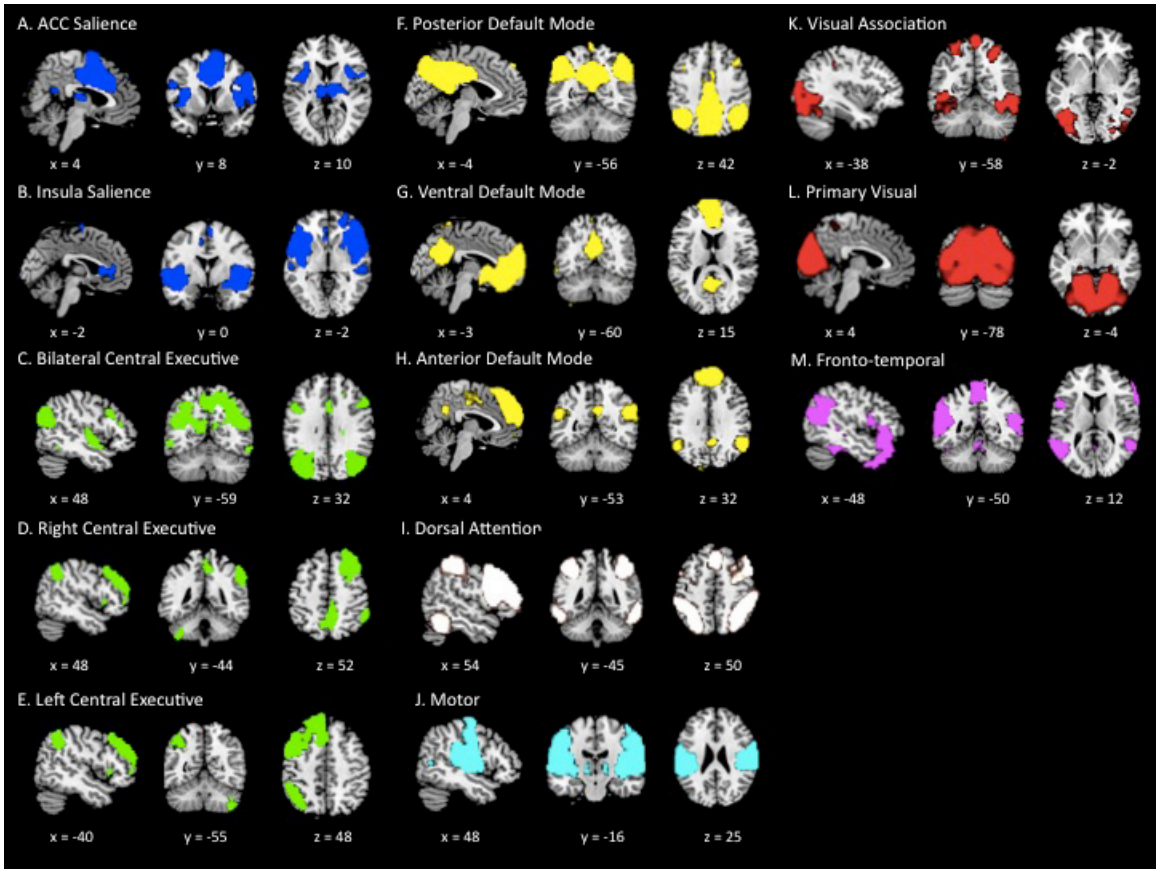

eFigure 4. Large-scale brain networks identified using ICA: Replication Cohort.

Data from thirty children (15 ASD, 15 TD) were combined in a group ICA to identify 25 independent components (networks) across all participants in a data-driven manner. Thirteen of these components correspond to previously identified functional networks: (a) ACC salience; (b) insula salience; (c) bilateral central executive; (d) right central executive; (e) left central executive; (f) posterior default mode; (g) ventral default mode; (h) anterior default mode; (i) dorsal attention; (j) motor, (k) visual association, (l) primary visual, and (m) fronto-temporal. Maps are displayed at $z > 2.3$, $p < 0.01$.

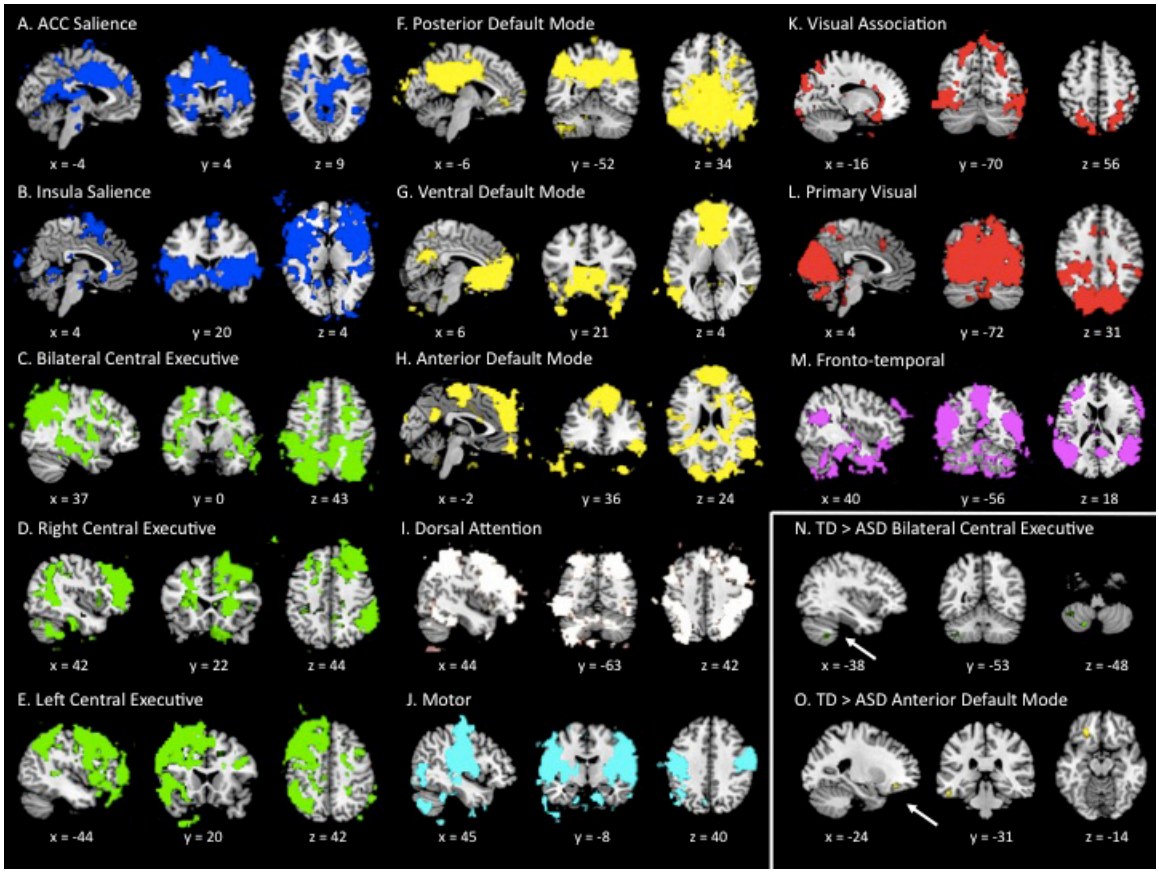

eFigure 5. Brain network hyper-connectivity in children with ASD: Replication Cohort. ASD > TD functional connectivity was observed in all of the networks examined: (a) ACC salience; (b) insula salience; (c) bilateral central executive; (d) right central executive; (e) left central executive; (f) posterior default mode; (g) ventral default mode; (h) anterior default mode; (i) dorsal attention; (j) motor, (k) visual association, (l) primary visual, and (m) fronto-temporal. A few extra-network voxels were observed in two networks: (n) bilateral central executive and (o) anterior default mode for the TD > ASD contrast. Group difference maps were thresholded using threshold-free cluster enhancement (TFCE) and $p < 0.05$.